Ann Surg Oncol (2017) 24:931–938
DOI 10.1245/s10434-016-5690-5

Annals of
SURGICAL ONCOLOGY
OFFICIAL JOURNAL OF THE SOCIETY OF SURGICAL ONCOLOGY

ORIGINAL ARTICLE – GASTROINTESTINAL ONCOLOGY

Preclinical Evaluation of Cathepsin-Based Fluorescent Imaging System for Cytoreductive Surgery

Carlos H. F. Chan, MD, PhD[1,2], Lukas F. Liesenfeld, MD[1], Isabel Ferreiro-Neira, PhD[1], and James C. Cusack Jr., MD[1]

[1]Department of Surgery, Massachusetts General Hospital, Boston, MA; [2]Department of Surgery, University of Iowa Carver College of Medicine, Iowa City, IA

ABSTRACT

Background. Cytoreductive surgery and hyperthermic intraperitoneal chemotherapy (CRS-HIPEC) is a treatment option for peritoneal surface malignancies. The ability to detect microscopic foci of peritoneal metastasis intraoperatively may ensure the completeness of cytoreduction. In this study, we evaluated the suitability of a hand-held cathepsin-based fluorescent imaging system for intraoperative detection of appendiceal and colorectal peritoneal metastasis.

Methods. Peritoneal tumors and normal peritoneal tissues were collected from patients with appendiceal and colorectal peritoneal metastasis. Expression of different cathepsins (CTS-B, -D, -F, -G, -K, -L, -O, and -S) was determined by quantitative RT-PCR and immunohistochemistry. The hand-held cathepsin-based fluorescent imaging system was used to detect peritoneal xenografts derived from human colon cancer cells (HT29, LoVo and HCT116) in nu/nu mice.

Results. While the expression levels of CTS-B, -D, -L, and -S could be higher in peritoneal tumors than normal peritoneum with a median (range) of 6.1 (2.9–25.8), 2.0 (1.0–15.8), 1.4 (0.8–7.0), and 2.1 (1.6–13.9) folds by quantitative RT-PCR, respectively, CTS-B was consistently the major contributor of the overall cathepsin expression in appendiceal and colonic peritoneal tumors, including adenocarcinomas and low-grade appendiceal mucinous neoplasms. Using peritoneal xenograft mouse models, small barely visible colonic peritoneal tumors (<2.5 mm in maximum diameter) could be detected by the hand-held cathepsin-based fluorescent imaging system.

Conclusions. Because cathepsin expression is higher in peritoneal tumors than underlying peritoneum, the hand-held cathepsin-based fluorescent imaging system could be useful for intraoperative detection of microscopic peritoneal metastasis during CRS-HIPEC and clinical trial is warranted.

Peritoneal surface malignancies include primary peritoneal malignant mesothelioma and peritoneal metastasis of various cancers. The presence and extent of disease often are difficult to be fully evaluated by noninvasive techniques, such as CT, PET, or MRI.[1] These imaging modalities are limited by their inability to detect small peritoneal nodules, which often are detected at the time of surgical exploration.[1] The presence of peritoneal metastases has significant negative impact on survival. Cytoreductive surgery and hyperthermic intraperitoneal chemotherapy (CRS-HIPEC) is a surgical treatment option for selected patients with peritoneal metastasis of appendiceal, colorectal, gastric, or ovarian cancers.[2–5] It involves surgical resection of all visible disease and intra-abdominal treatment with hyperthermic chemotherapy. One of the most important determinants of treatment success and long-term overall and disease-free survival is the ability to achieve complete cytoreduction.[2–5] While patients with no residual disease (CCR0) or minimal residual peritoneal surface tumor nodules less than 2.5 mm in maximum

Carlos H. F. Chan and Lukas F. Liesenfeld have contributed equally to this work.

Electronic supplementary material The online version of this article (doi:10.1245/s10434-016-5690-5) contains supplementary material, which is available to authorized users.

First Received: 12 May 2016;
Published Online: 2 December 2016

C. H. F. Chan, MD, PhD
e-mail: carloshfchan@gmail.com

J. C. Cusack Jr., MD
e-mail: jcusack@mgh.harvard.edu

diameter (CCR1) have significantly better survival than those with residual nodules more than 2.5 mm in maximum diameter (CCR2), patients with CCR0 have the best outcome.[2–4]

To enhance our ability to achieve complete cytoreduction at the time of CRS, we propose to use a novel fluorescent imaging system (LUM Imaging System, Lumicell, Inc.), which has been developed for intraoperative cancer detection using a cathepsin-activatable fluorescent nanoparticle (LUM015) along with a near-infrared detection device (LUM Imaging Device).[6] Many types of cancer cells express a higher level of cathepsin proteases than normal cells.[7] In the presence of cathepsins, the quencher portion of LUM015 can be released from the nanoparticle allowing its fluorescence to be detected by the LUM Imaging Device.[6] The LUM Imaging System has been tested successfully on preclinical animal models of sarcomas.[6,8–10] A Phase 1 clinical study in sarcoma and breast cancer patients ($N = 15$) showed no observable adverse events related to LUM015 (ClinicalTrials.gov identifier: NCT01626066).[6] This system is currently being evaluated in a phase 2 feasibility study for assessing surgical margins during breast cancer surgery (ClinicalTrials.gov identifier: NCT02438358).

Human cathepsin family consists of 12 cysteine cathepsins (CTS-B, -C, -F, -H, -L, -K, -O, -S, -V, -W, -X, and -Z), 2 aspartic cathepsins (CTS-D and -E) and 2 serine cathepsins (CTS-A and -G), which have different expression patterns and biological functions related to their protease activity.[11] Higher expression levels of CTS-B, -D, -L, and -S have been reported in human colorectal tumors in comparison to normal colonic mucosa.[12–17] Cathepsin expression in appendiceal neoplasms, including adenocarcinoma, goblet cell carcinoid (GCC) and low-grade appendiceal mucinous neoplasm (LAMN), has not been reported in the literature. In this study, we aim to determine the cathepsin expression in appendiceal and colorectal peritoneal metastatic tumors and to evaluate the use of LUM Imaging System in a preclinical animal model for intraoperative detection of peritoneal metastasis.

MATERIALS AND METHODS

Cell Lines and Cell Culture

Human colorectal cancer cell lines (HT29, LoVo, and HCT116) were purchased from the American Type Culture Collection (ATCC). HT29, LoVo, and HCT116 cells were maintained using DMEM, F-12 K, and McCoy (GIBCO), respectively, supplemented with 10% fetal bovine serum (GIBCO), 100 U/ml penicillin, and 10 µg/ml streptomycin (Invitrogen) in a humidified atmosphere of 5% CO_2 at 37 °C.

Animal and Peritoneal Xenograft Model

Six week-old female nu/nu mice (CrTac:NCr-*Foxn1*^{nu}) were purchased from Taconic Biosciences. With approval of the Institutional Animal Care and Use Committee, 2×10^6 human colorectal cancer cells were injected intraperitoneally and incubated for 2–4 weeks for in vivo peritoneal tumor imaging studies.

Patient Population and Tissue Collection

With approval of the Institution Review Board, peritoneal tissues were collected from consented patients, who were undergoing CRS-HIPEC for colorectal or appendiceal peritoneal surface malignancies at MGH between January and April 2015. Normal peritoneal tissues and solid portion of peritoneal tumors were resected and processed immediately for formalin-fixed tissue blocks and frozen tissues.

cDNA Preparation and Quantitative RT-PCR

RNAs were extracted from frozen peritoneal tissues using the RNeasy fibrous tissue mini kit (QIAGEN), per manufacturer's instructions. Purified RNAs were reverse-transcribed using the ThermoScript™ RT-PCR System for First-Strand cDNA Synthesis (Life Technologies) per manufacturer's instructions. Quantitative PCR was performed using the LightCycler® 96 System (Roche) with individual purified cDNA, Fast SYBR Green Master Mix (Life Technologies), and primer sets specific for human cathepsin genes (Supplemental methods). Three internal reference genes (HSPCB, YWHAZ and RPS13) were selected and used according to the study published by Jacob et al.[18] Melting curves for all qPCR reactions were verified to ensure single specific products. Expression levels of cathepsins were normalized with all three reference genes to ensure reliable comparisons.

Peritoneal Tumor Detection and Image Analysis

After incubating human colorectal cancer cells for 2–4 weeks in nu/nu mouse peritoneal cavity, 150 µl of 26.7 µM LUM015 imaging agent (Lumicell, Inc.) was injected intravenously via its tail vein. Six hours after administration, the mouse abdominal cavity was opened. The entire peritoneal surface was examined visually for peritoneal nodules and systemically scanned using the handheld LUM 2.6 Imaging Device (Lumicell, Inc.). To remove the background fluorescence emitted from the mouse skin, only abdominal wall was used for imaging analysis. Fluorescent images were taken at the time of exploration and processed using ImageJ software for

quantification. Mean fluorescent level of individual peritoneal tumor (a field outlining the entire tumor) was compared to the one of adjacent normal peritoneum (an average value calculated from five random fields of ~10,000 pixels).

Immunohistochemistry

Paraffin-embedded, formalin-fixed tissue sections were deparaffinized using xylene and rehydrated per standard protocol. Heat induced epitope retrieval was performed in microwave oven with Tris/EDTA buffer (10 mM Tris base, 1 mM EDTA, 0.05% Tween-20, pH 9.0). After cooling, tissue sections were blocked with 3% bovine serum albumin in TBS buffer (50 mM Tris–Cl, 150 mM NaCl, pH 7.6). Tissue sections were incubated with primary rabbit antibodies specific for cathepsin B (FL-399, Santa Cruz Biotechnology), cathepsin L (H-80, Santa Cruz Biotechnology) and cathepsin D (H-75, Santa Cruz Biotechnology) at a concentration of 1:100 dilutions at room temperature for 1 h. Endogenous peroxidases were then inactivated by 3% hydrogen peroxide. After washing with TBS buffer, tissue sections were incubated with secondary HRP-conjugated polyclonal goat anti-rabbit antibodies (P0448, DAKO) at room temperature for 30 min in the dark. After washing with TBS buffer, tissue sections were incubated with DAB + Chromogen (3,3′-diaminobenzidine, K3467, DAKO) for 3 min, counterstained with Mayer's Hematoxylin Lillie's Modification (DAKO) for 2 min and blued in running tap water for 10 min. Negative controls were performed without primary antibodies at the same time.

Statistical Methods

For quantitative RT-PCR, relative cathepsin expression levels for the pooled samples were compared with two-tailed Student's t tests. P value <0.05 was considered statistically significant. For imaging analysis, 95% confidence intervals (CI) of tumor-to-normal peritoneum relative fluorescent intensities were calculated. Statistical significance was considered if the lower CI limit was above 1. Receiver operating characteristic (ROC) curve was constructed using SPSS Statistics software with different signal threshold on normal peritoneum and peritoneal tumors.

RESULTS

Cathepsin Expression in Appendiceal and Colorectal Peritoneal Metastatic Tumors

Human colorectal cancers can produce higher levels of cathepsin B, D, L, and S.[12–17] However, reports on their expression in peritoneal metastasis and appendiceal neoplasms are lacking. We tested the expression in eight patients with peritoneal tumors (0.5–2 cm) of colonic ($n = 2$) and appendiceal ($n = 6$) origin (Table 1). A total of nine adenocarcinomas, four LAMNs, and three normal peritoneal tissues were tested. Using quantitative RT-PCR, the expression levels of CTS-B, -D, -L, and -S in peritoneal tumors were higher than normal peritoneum (Fig. 1), although statistical significance was not achieved due to a small sample size and variation in expression levels among tumors (Supplementary Fig. 1). Nevertheless, CTS-B was consistently expressed above normal peritoneal level with a median of 6.1-fold (range 2.9–25.8) in both adenocarcinoma and LAMN (Supplementary Fig. 1). The expression levels of CTS-D, -L and -S were less consistent with a median of 2.0-fold (range 1.0–15.8), 1.4-fold (range 0.8–7.0), and 2.1-fold (range 1.6–13.9) higher, respectively (Supplementary Fig. 1). Consistent with the studies on primary colorectal tumors, CTS-B was the dominant cathepsin expressed in colorectal peritoneal metastatic tumors as well as in different appendiceal neoplasms, including LAMN, adenocarcinoma ex GCC, and mucinous adenocarcinoma (Fig. 1).[12–17] Only tumors from two patients (patients 1 and 5) had CTS-D and CTS-L expressed at a comparable level than CTS-B, respectively. Hence, CTS-B could be the main contributor for the overall cathepsin activity in these peritoneal tumors.

In terms of localization, CTS-B, -D, and -L were expressed primarily in the neoplastic cells and immune infiltrates by immunohistochemistry (Fig. 2). There was a strong contrast between cancer cells and stromal cells in adenocarcinomas but less in LAMN. This could explain the variability in terms of expression levels by quantitative RT-PCR among tumors. The tumors with the highest cancer cell component, such as the adenocarcinoma ex GCC shown (Fig. 2), would have the highest cathepsin expression level (Supplementary Fig. 1). Although the overall cathepsin activity in peritoneal tumors could be influenced by their tissue composition, all the tumors tested had higher overall cathepsin expression than normal peritoneum.

Detection of Peritoneal Xenografts using the LUM Imaging System

The expression of different cathepsins in peritoneal xenografts derived from HT29, LoVo, and HCT116 cells was determined by quantitative RT-PCR and immunohistochemistry. Using quantitative RT-PCR with primers specific for human cathepsin genes, the expression levels of human CTS-B and -D were significantly higher than other cathepsins tested in HT29, LoVo, and HCT116 tumors (Fig. 3, $P < 0.01$). Using immunohistochemistry with antibodies recognizing both human and mouse cathepsins,

TABLE 1 Patient characteristics

Patient	Age/gender	Primary site	Pathology	No. of tumors	Cathepsin[a]
1	51/F	Cecum	Poorly differentiated adenocarcinoma with mucinous and signet ring features	1	**B**, **D**, S
2	71/F	Ascending Colon	Moderately differentiated adenocarcinoma	1	**B**, D, S
3	43/M	Appendix	Intermediate-grade mucinous adenocarcinoma	3	**B**, S
4	44/M	Appendix	Low-grade mucinous adenocarcinoma	1	**B**, D, L
5	55/M	Appendix	Low-grade mucinous adenocarcinoma	2	**B**, **L**, S
6	56/M	Appendix	Adenocarcinoma ex goblet cell carcinoid	1	**B**, D, L, S
7	57/F	Appendix	Low-grade mucinous neoplasm	2	**B**, L, S
8	72/M	Appendix	Low-grade mucinous neoplasm	2	**B**, D, L

[a] Tumor-to-normal peritoneal cathepsin expression ratio ≥2. Bold letters represent dominant cathepsin(s) expressed (≥two-fold compared with other cathepsins)

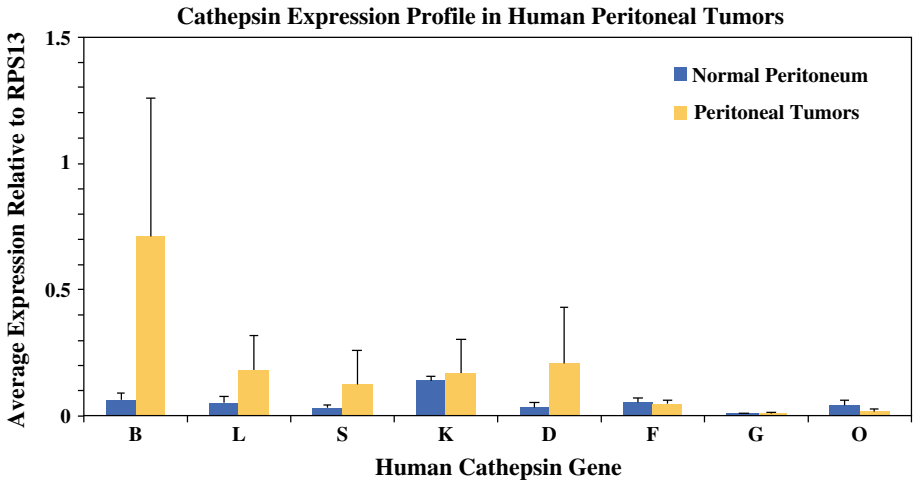

FIG. 1 Cathepsin expression in peritoneal tumors collected from patients. Expression levels of different human cathepsin genes (CTS-B, -L, -S, -K, -D, -F, -G, and -O) were quantified in normal peritoneum (*blue columns*) and peritoneal tumors (*yellow columns*) collected from patients using quantitative RT-PCR and normalized with RPS13 gene expression. Each column represents the average relative expression of individual cathepsin gene detected in normal peritoneum ($N = 3$) or peritoneal tumors ($N = 13$). *Error bars* represent standard deviation. CTS-B, -D, -L, and -S are expressed at a higher level in tumors than normal peritoneum

CTS-B, -D, and -L were all detected in the peritoneal tumors at a level higher than the underlying mouse abdominal wall (Supplementary Fig. 2). Although the absolute gene expression level of cathepsins could not be compared quantitatively between xenografts and underlying mouse peritoneum due to species difference, these peritoneal xenograft models could represent a good testing model for the LUM Imaging System.

The LUM Imaging System was previously shown to detect microscopic disease at the resection margin in various sarcoma animal models.[6,8–10] Using the recommended dose of LUM015 and treatment time point, fluorescent peritoneal tumors (< 2.5 mm in maximum diameter) of HT29, LoVo, and HCT116 could readily be detected by the handheld LUM Imaging Device above the background fluorescence signal from the normal abdominal wall (Fig. 4).[6] In mice without LUM015 injection, background fluorescence was minimal (data not shown). Using ImageJ software, tumor fluorescent levels were quantified and normalized with fluorescent background of adjacent normal abdominal wall. All average normalized tumor fluorescent levels with 95% confidence intervals were significantly above 1 (Supplementary Fig. 3). Using different detection threshold (pixel intensity: 70–110), specificity and sensitivity of the device ranged from 71–90% to 70–88%, respectively. The area under the curve in the ROC curve was 0.919 (Asymptotic 95% confidence interval: 0.886–0.952, $P < 0.001$; Fig. 4).

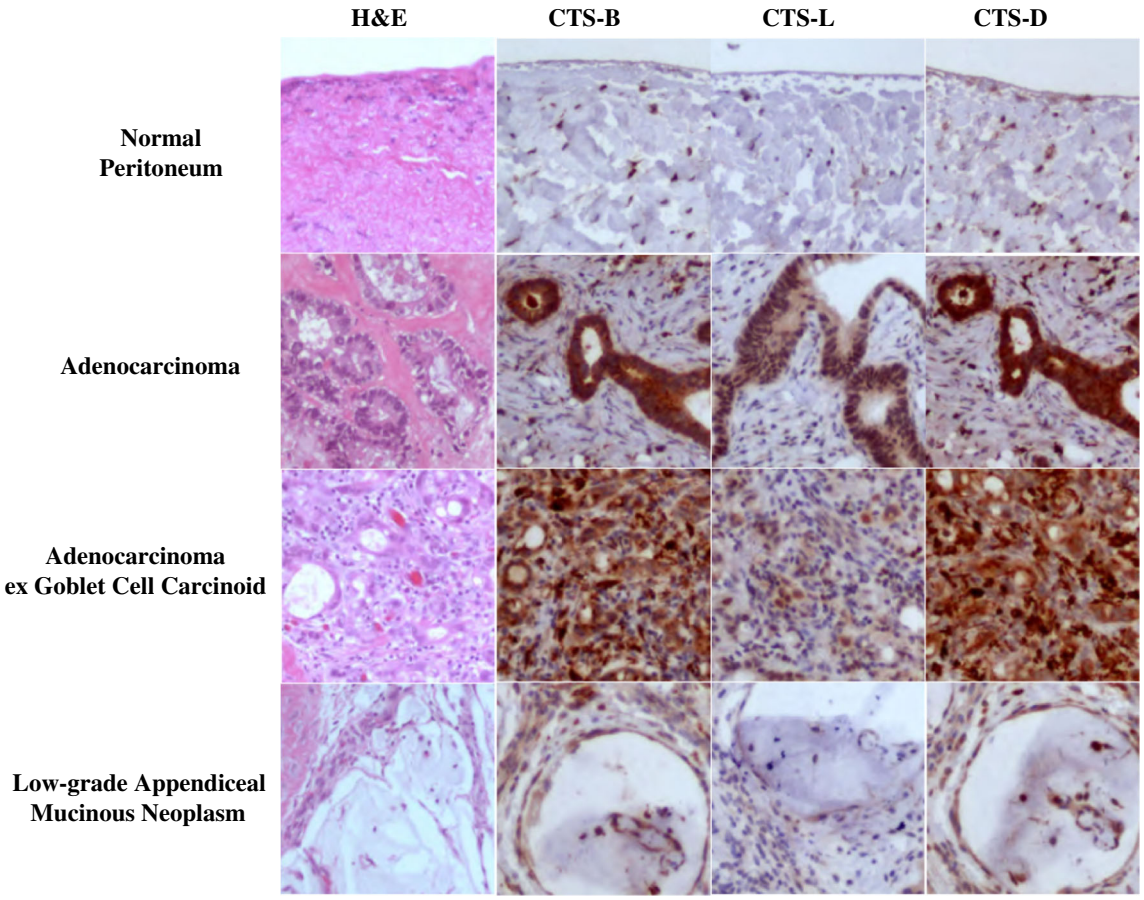

FIG. 2 Immunohistochemistry for cathepsins in peritoneal tumors collected from patients. Hematoxylin and eosin (H&E), cathepsin B (CTS-B), cathepsin L (CTS-L), and cathepsin D (CTS-D) staining are shown for normal peritoneum, adenocarcinoma, adenocarcinoma ex goblet cell carcinoid, and low-grade appendiceal mucinous neoplasm. Cathepsins were mainly detected in tumor cells and immune cells

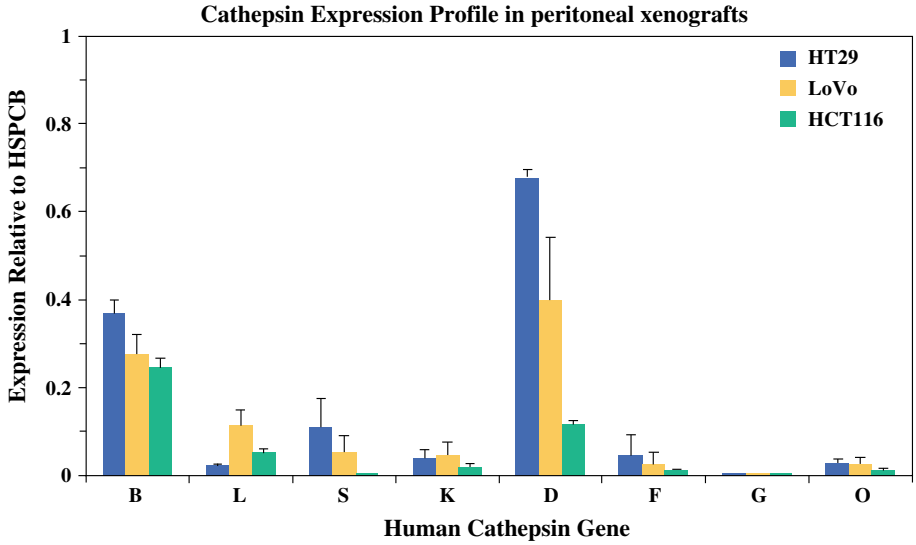

FIG. 3 Cathepsin expression in peritoneal xenografts of human colon cancer cells. Expression levels of different human cathepsin genes (CTS-B, -L, -S, -K, -D, -F, -G, and -O) were quantified in peritoneal tumors of HT29 (*blue columns*), LoVo (*yellow columns*), and HCT116 (*green columns*) cells using quantitative RT-PCR and normalized with human HSPCB gene expression. Primers were specific to human genes only. Each column represents the average relative expression of individual cathepsin gene detected in three tumors. *Error bars* represent standard deviation. CTS-B and -D are the predominant cathepsins expressed

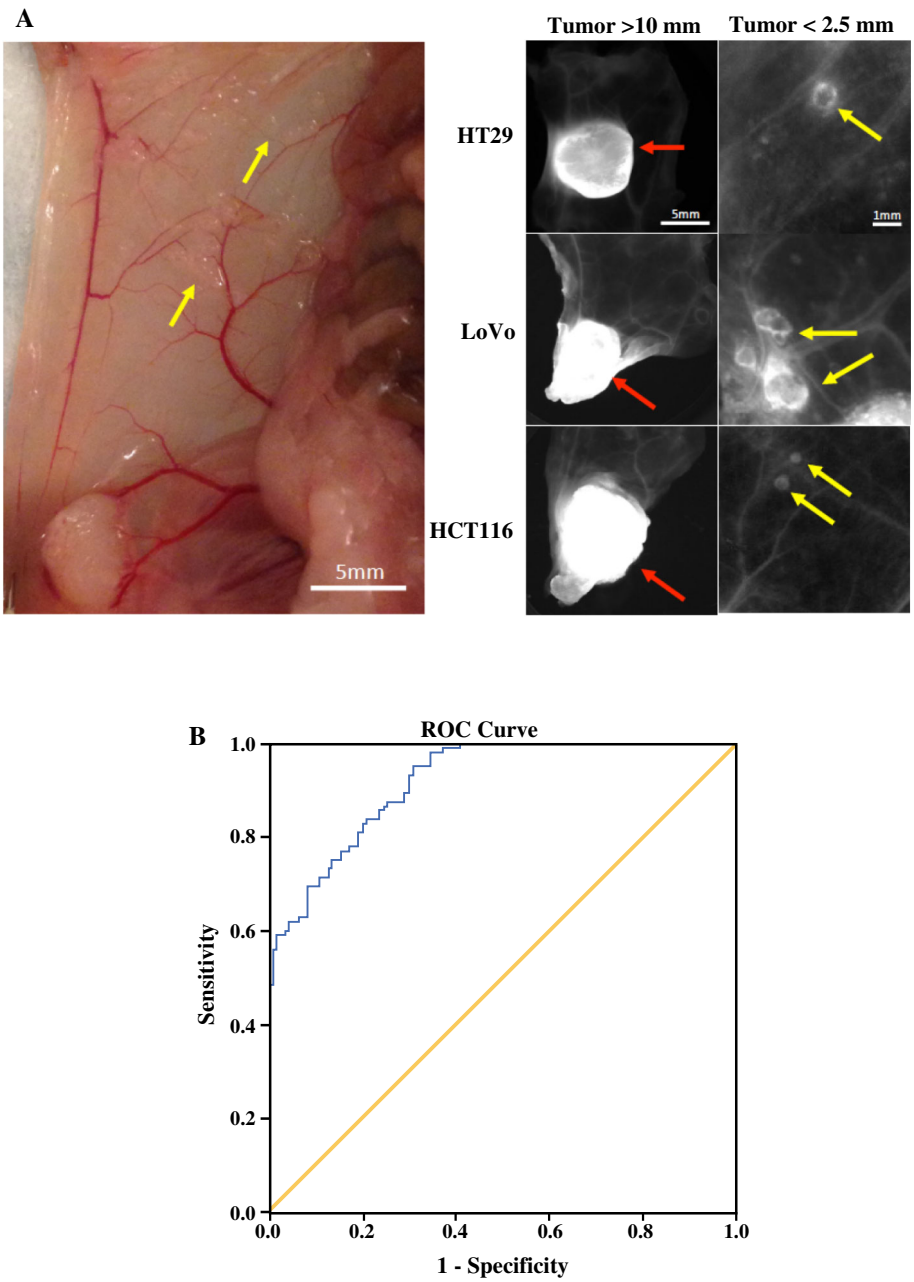

FIG. 4 Detection of peritoneal xenografts using LUM Imaging System. **a** Peritoneal cavity of a nu/nu mouse bearing numerous peritoneal tumors (*yellow arrows*). White bar represents a scale of 5 mm (*left panel*). Six hours after tail vein injection of LUM015, fluorescent peritoneal tumors of HT29, LoVo, and HCT116 were detected by the handheld LUM 2.6 Imaging Device. Large tumors (>10 mm, *left panel*, *red arrows*) and small tumors (<2.5 mm, *right panel*, *yellow arrows*) were detected from the background of normal abdominal wall. At least three mice were evaluated per cell line (*right panel*). **b** ROC curve constructed using different detection threshold on both normal peritoneum and peritoneal tumors. *Blue line* LUM imaging system; *yellow line* hypothetical line for an uninformative test. Area under the curve (AUC) was 0.919 (asymptotic 95% confidence interval: 0.886–0.952, $P < 0.001$)

DISCUSSION

Cathepsins belong to a group of proteases that have been shown to be involved in cancer progression and can be overexpressed in various cancers, including colorectal cancers.[19–22] Consistent with the literature, we have shown that CTS-B, -D, and -S can be detected in colorectal adenocarcinomas. Moreover, we have shown the expression of CTS-B, -D, -L, and -S in different appendiceal neoplasms for the first time. In contrast to other cathepsins tested, CTS-B is the only one consistently and dominantly expressed in all the adenocarcinomas originated from the appendix and colon as well as in LAMN. CTS-B has been shown to promote cancer cell proliferation, tumor growth, angiogenesis, invasion, and organ metastasis.[22] Although its role in peritoneal metastasis remains to be elucidated, it may represent a potential therapeutic target for appendiceal or colorectal peritoneal metastasis.

Fluorescence imaging technology has been evaluated to detect sentinel lymph nodes and assess margin status in patients with breast cancers, to detect sentinel lymph nodes in patients with rectal cancers, and to guide surgery for brain tumors.[23–28] This fluorescence imaging technology uses indocyanine green (ICG) or fluorescein, which are not tumor-specific, and relies on the presence of vascular or lymphatic channels. Nevertheless, recent studies have

suggested its utility on peritoneal carcinomatosis of colorectal cancer and hepatocellular carcinoma.[29,30] In the study by Liberale et al., high sensitivity and specificity have been reported for non-mucinous peritoneal tumors of colorectal adenocarcinomas using ICG fluorescent imaging; but none of the mucinous tumors have any fluorescent signal limiting its use in mucinous neoplasms.[29] Moreover, it is unclear regarding the size of peritoneal tumors evaluated in their study.[29] The reported sensitivity and specificity may not necessarily apply to peritoneal tumors <2.5 mm in size, which often have limited vascular supply; hence, this probably limits its use to improve the quality of cytoreductive surgery. Unlike those studies using ICG, the LUM Imaging System uses a cathepsin-activatable probe, LUM015. Because tumors express cathepsins at a higher level than normal tissues, the fluorescent signal is more tumor-specific as demonstrated in the study conducted by Whitley et al.[6] They have shown that LUM015 is activated and accumulated in the tumors, making the agent more tumor-specific compared with adjacent normal tissues.[6] In our study, we have shown the utility of the LUM Imaging System in detecting small peritoneal tumors (<2.5 mm) in the colonic peritoneal xenograft model. The ability of detecting and potentially eradicating these small peritoneal tumors may improve the completeness of cytoreduction before HIPEC, which may subsequently improve the clinical outcome in patients with peritoneal surface malignancies.

Although our study shows some promising results supporting the use of LUM Imaging System for intraoperative detection of peritoneal metastasis, there are some limitations. (1) We have limited number of samples per histological subtype. Appendiceal neoplasms are rare and comprised of a variety of histological types. Patients with colorectal peritoneal metastasis are more common, but most of them are not eligible for CRS-HIPEC. Nevertheless, this collection represents our patient population, which will be the target population for the upcoming clinical trial. (2) The peritoneal xenograft mouse models may not be truly representative to the actual patients. The pharmacokinetics and pharmacodynamics of LUM015 in peritoneal tumors may be different. The fluorescent background may not be comparable between human and mouse peritoneal cavity. We have not tested on mice with appendiceal peritoneal tumors due to the lack of available model. Nonetheless, the most appropriate evaluation of this imaging system for detecting peritoneal metastasis is in a human clinical trial setting.

In conclusion, we have shown here cathepsin expression can be higher in both appendiceal and colonic peritoneal tumors than in normal peritoneum and the LUM Imaging System can be used to detect colonic peritoneal xenografts. Although these preclinical data support the use of LUM Imaging System in this clinical setting, clinical trials will be required to ensure appendiceal and colorectal peritoneal metastatic tumors can be identified by the LUM Imaging System, to estimate its specificity and sensitivity, and to assess the impact on patient outcome; none of these can be obtained from preclinical animal models. This imaging system has the potential to guide CRS-HIPEC and to detect occult peritoneal metastasis during surgery for operable diseases.

ACKNOWLEDGEMENT The authors thank Lumicell, Inc. for providing the LUM015 imaging agent and the LUM Imaging Device.

AUTHORS' CONTRIBUTION CH.F.C. contributed to the conception, design, data collection, data analysis, and article preparation. L.F.L. contributed to the design, data collection, data analysis, and article review. I.F. contributed to data analysis and article review. J.C.C. contributed to the conception and article review.

DISCLOSURE CH.F.C., L.F.L., I.F., and J.C.C. report neither any disclosure nor any financial support.

REFERENCES

1. Valle M, Federici O, Garofalo A. Patient selection for cytoreductive surgery and hyperthermic intraperitoneal chemotherapy, and role of laparoscopy in diagnosis, staging, and treatment. *Surg Oncol Clin N Am*. 2012;21:515–32.
2. Votanopoulos KI, Shen P, Stewart IV JH, Levine EA. Current status and future directions in appendiceal cancer with peritoneal dissemination. *Surg Oncol Clin N Am*. 2012;21:599–610.
3. Elias D, Quenet F, Goere D. Current status and future directions in the treatment of peritoneal dissemination from colorectal carcinoma. *Surg Oncol Clin N Am*. 2012;21:611–24.
4. Glockzin G, Piso P. Current status and future directions in gastric cancer with peritoneal dissemination. *Surg Oncol Clin N Am*. 2012;21:625–34.
5. Helm CW. Current status and future directions of cytoreductive surgery and hyperthermic intraperitoneal chemotherapy in the treatment of ovarian cancer. *Surg Oncol Clin N Am*. 2012;21:645–64.
6. Whitley MJ, Cardona DM, Lazarides AL, et al. A mouse-human phase 1 co-clinical trial of a protease-activated fluorescent probe for imaging cancer. *Sci Transl Med*. 2016:8:320ra4.
7. Mohamed MM, Sloane BF. Cysteine cathepsins: multifunctional enzymes in cancer. *Nat Rev Cancer*. 2006;6:764–75.
8. Mito JK, Ferrer JM, Brigman BE, et al. Intraoperative detection and removal of microscopic residual sarcoma using wide-field imaging. *Cancer*. 2012;118;5320–30.
9. Eward WC, Mito JK, Eward CA, et al. A novel imaging system permits real-time in vivo tumor bed assessment after resection of naturally occurring sarcomas in dogs. *Clin Orthop Relat Res*. 2013;471:834–42.
10. Cuneo KC, Mito JK, Javid MP, et al. Imaging primary mouse sarcomas after radiation therapy using cathepsin-activatable fluorescent imaging agents. *Int J Radiat Oncol Biol Phys*. 2013;86:136–42.
11. Tan G, Peng Z, Lu J, Tang F. Cathepsins mediate tumor metastasis. *World J Biol Chem*. 2013;4:91–101.
12. Chauhan SS, Goldstein LJ, Gottesman MM. Expression of cathepsin L in human tumors. *Cancer Res*. 1991;51:1478–81.

13. Shuja S, Sheahan K, Murnane MJ. Cysteine endopeptidase activity levels in normal human tissues, colorectal adenomas and carcinomas. *Int J Cancer*. 1991;49:341–6.
14. Campo E, Munoz J, Miquel R, et al. Cathepsin B expression in colorectal carcinomas correlates with tumor progression and shortened patient survival. *Am J Pathol*. 1994;145:301.
15. Adenis A, Huet G, Zerimech F, Hecquet B, Balduyck M, Peyrat JP. Cathepsin B, L, D activities in colorectal carcinomas: relationship with clinic-pathological parameters. *Cancer Lett*. 1995;96:267–75.
16. Mayer A, Fritz E, Fortelny R, Kofler K, Ludwig H. Immunohistochemical evaluation of cathepsin D expression in colorectal cancer. Cancer Invest. 1997;15:106–110.
17. Gormley JA, Hegarty SM, O'Grady A, et al. The role of Cathepsin S as a marker of prognosis and predictor of chemotherapy benefit in adjuvant CRC: a pilot study. *Br J Cancer*. 2011;105:1487–94.
18. Jacob F, Guertier R, Naim S, et al. Careful selection of reference genes is required for reliable performance of RT-qPCR in human normal and cancer cell lines. *PLoS ONE*. 2013;8:e59180.
19. Sulpizio S, Franceschini N, Piattelli A, Di Sebastiano P, Innocenti P, Selvaggi F. Cathepsins and pancreatic cancer: the 2012 update. *Pancreatology*. 2012;12:395–401.
20. Tan GJ, Peng ZK, Lu JP, Tang FQ. Cathepsins mediate tumor metastasis. *World J Biol Chem*. 2013;4:91–101.
21. Olson OC, Joyce JA. Cysteine cathepsin proteases: regulators of cancer progression and therapeutic response. *Nat Rev Cancer*. 2015;15:712–29.
22. Aggarwal N, Sloane BF. Cathepsin B: multiple roles in cancer. *Proteomics Clin Appl*. 2014;8:427-37.
23. Pleijhuis RG, Langhout GC, Helfrich W, et al. Near-infrared fluorescence (NIRF) imaging in breast-conserving surgery: assessing intraoperative techniques in tissue-simulating breast phantoms. *Eur J Surg Oncol*. 2011;37:32–9.
24. Stoffels I, Dissemond J, Pöppel T, Schadendorf D, Klode J. Intraoperative fluorescence imaging for sentinel lymph node detection: prospective clinical trial to compare the usefulness of indocyanine green vs technetium Tc 99m for identification of sentinel lymph nodes. *JAMA Surg*. 2015;150:617–23.
25. Noura S, Ohue M, Seki Y, et al. Feasibility of a lateral region sentinel node biopsy of lower rectal cancer guided by indocyanine green using a near-infrared camera system. *Ann Surg Oncol*. 2010;17:144–51.
26. Handgraaf HJ, Boogerd LS, Verbeek FP, et al. Intraoperative fluorescence imaging to localize tumors and sentinel lymph nodes in rectal cancer. *Minim Invasive Ther Allied Technol*. 2016;25:48–53.
27. Liberale G, Vankerckhove S, Galdon MG, Donckier V, Larsimont D, Bourgeois P. Fluorescence imaging after intraoperative intravenous injection of indocyanine green for detection of lymph node metastases in colorectal cancer. *Eur J Surg Oncol*. 2015;41:1256–60.
28. Kabuto M, Kubota T, Kobayashi H, et al. Experimental and clinical study of detection of glioma at surgery using fluorescent imaging by a surgical microscope after fluorescein administration. *Neurol Res*. 1997;19:9–16.
29. Liberale G, Vankerckhove S, Galdon MG, et al. Fluorescence imaging after indocyanine green injection for detection of peritoneal metastases in patients undergoing cytoreductive surgery for peritoneal carcinomatosis from colorectal cancer. *Ann Surg*. 2016.
30. Satou S, Ishizawa T, Masuda K, et al. Indocyanine green fluorescent imaging for detecting extrahepatic metastasis of hepatocellular carcinoma. *J Gastroenterol*. 2013;48:1136–43.